

GEOMETRIC CHARACTERIZATION OF THE SHADOWCAM INSTRUMENT. E.J. Speyerer¹, R.V. Wagner¹, M.S. Robinson¹, P. Mahanti¹, and D. Humm², ¹Arizona State University, Tempe, AZ, ²SPICACON, Annapolis, MD.

Introduction: The ShadowCam instrument on Danuri, also referred to as the Korean Pathfinder Lunar Orbiter (KPLO), was launched on 5 August 2022. ShadowCam is a NASA-contributed instrument designed to increase our understanding of volatiles in the lunar polar regions by addressing a series of Strategic Knowledge Gaps (SKGs) [1]. The design of the ShadowCam instrument has a high heritage from the Lunar Reconnaissance Orbiter Camera (LROC) Narrow-Angle Cameras (NACs) [2], which have acquired over 1.75 million images of the lunar surface since entering orbit around the Moon in June 2009. The optical assembly consists of hyperbolic primary and secondary mirrors (Richey-Chretien) with a field of view of approximately 3° and an f-stop of 3.6. The sunshade contains a series of inner baffles to reduce the scattered light within the instrument to limit stray light from nearby sun-illuminated surfaces (Fig. 1). A Time Delay Integration (TDI) sensor from Hamamatsu Photonics replaced the original line array sensor in the LROC NAC instrument to increase the number of photons captured in an observation from the reflected light within the PSR without affecting the spatial resolution of the final image. In addition, the electronics enable readout from both sides of the detector, allowing the capture of images in both flight orientations.

Through a series of pre-flight and now in-flight experiments (not covered in this abstract), we have characterized the geometry of the ShadowCam instrument. This enables precise mapping of individual surface features, which is needed to meet the above objectives. Unlike typical imaging of directly illuminated terrain, which has a single set of photometric angles (incidence, emission, phase), the diffuse, scattered light source inside PSRs creates a complex lighting geometry with multiple photometric angles contributing to the illumination within the PSR. Therefore, numerous co-registered observations are needed to interpret the geology of a single point on the surface.

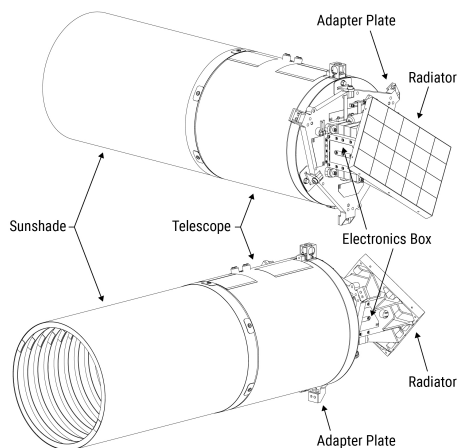


Figure 1: Technical drawing of ShadowCam

Sensor Geometry: ShadowCam uses a Time-Delay Integration (TDI) Charged Couple Device (CCD) provided by Hamamatsu Photonics (S10202-08-01) to collect photons reflected out of permanent and temporarily shadowed regions. Unlike the NAC instrument, which consists of a single 5001×1 -pixel array that collects single-line integrations and uses the motion of the spacecraft to build an image, the TDI CCD collects multiple integrations over a single pass across the surface. The shape of the detector accomplishes this. The Hamamatsu detector in ShadowCam is 4096 pixels across and has 128 lines, also called TDI stages. The 4096 pixels are split across eight 512-pixel channels, of which ShadowCam uses the center six due to constraints of the optics (*Total active pixels*=3072).

As an object enters the camera field of view, the feature is imaged by the first active stage of the TDI detector. As the instrument scans across the surface, the charge from the first stage of the TDI is transferred to the next stage, and additional photons from the object are captured and add it to the signal in the CCD. This process is repeated for all the following stages on the detector until the charge reaches the horizontal read buffer at the end of all 128 stages. The serial buffer then transfers the charge to the Analog-to-Digital (A2D) converter, which converts the analog signal (electrons) to a digital number (DN). Before reaching the A2D converter, the signal from the horizontal buffer travels through eight physical pixels on the detector that move the charge away from the imaging portion of the sensor such that the eight channels are adjacent to one another without any gaps in spatial coverage.

Image Geometry: A raw ShadowCam image contains 3144 samples or 524 pixels per channel. Of the 524 pixels, 512 are active and sensitive to incoming photons. The remaining twelve pixels are used solely for calibration purposes. Each line in each channel has ten prescan pixels and two overscan pixels. These pre- and overscan pixels are typically used to characterize the bias level of the observation. The bias should have $DN > 0$ to ensure a linear response to the incoming light. As stated above, the sensor contains eight physical pixels between the first active pixel and the A2D converter. Therefore, two of the prescan pixels in the raw images are virtual pixels. Virtual pixels are generated by sampling the A2D converter without clocking the horizontal read buffer. Likewise, the sensor contains no physical pixels beyond the active array, indicating that the two overscan pixels in the images are also virtual. In the ideal case, all twelve pixels would sample the bias level of the observation. However, in our current implementation of the radiometric calibration, we only use the eight physical pre-scan pixels to characterize the bias level since some residual charge has been observed in the two overscan pixels when targeting bright scenes.

While the image width is the same for all observations, the length of the image can vary depending on the objectives of the acquisition. Additionally, in most cases, the first line of the raw

image may not be the first line read by the electronics. Each observation has a commanded number of preroll lines that are acquired but thrown out and not saved in the raw image. We typically use 1024 lines of preroll, but in some cases, calibration images are acquired with as little as zero preroll lines. In this ladder case, the signal contained in the detector before the observation may be stored in the first 128 lines of the raw image.

Optical Distortion: With an understanding of the sensor and image geometry, it is now possible to explore the optical system's geometric distortions. Before flight, the camera was calibrated at MSSS. Since the camera system is focused on infinity, it is impossible to image a standard calibration target directly and still be in focus. Instead, the camera is positioned in front of a set of optics with the same prescription as the ShadowCam instrument. This enables imaging of a target in focus. For the geometric characterization, we used a tilted bar target. The illuminated bar target has a set of equally sized opaque bars. Several filled-in bars offer unique signatures in the raw images to supply some reference to where you are along the set of uniform bars. One way to measure the distortion would be to measure the width of the individual bars. However, this method assumes that all the bars are the same width and fails to provide a dense and robust set of measurements to quantify small-scale distortions.

Alternatively, the interior orientation parameters (i.e., principal point, focal length, and optical distortion) were characterized using a collimator projecting a tilted bar target while the camera was mounted on an Ultradex rotary stage that provided accurate azimuthal control in one-degree increments. Since the field of view of the ShadowCam instrument is narrow ($\sim 3^\circ$) with respect to the increments available on the rotary stage, multiple sets of observations were recorded. Between each image set, the rotary stage was moved on the table in an uncontrolled manner, after which a new set of measurements was acquired. These random realignments enabled the bar pattern to be viewed in different portions of the detector, thus measuring the optical properties of the camera over a broader area.

The tilted bar pattern target meant that the projected image was in focus at one point and went out of focus near the edges. Twenty sets of three to four calibration images of the bar target were acquired. The camera was accurately adjusted one degree between each image, causing the bar pattern to shift across the detector. We then analyzed how far the bars moved after the one-degree rotation to derive the interior orientation parameters. We removed the prescan and overscan pixels from each channel, creating an image of 3072 pixels wide (512x6). We then applied a 9-pixel wide Gaussian filter (sigma=1.76) to find the bar edge at the sub-pixel level. We calculated the absolute value of the derivative along each line of the image. With this filtering applied, the edge of the bar target was identified with a spike in the signal. We found the peak location associated with the bar's edge from this signal. To accurately find the peak to a sub-pixel level, we selected the two neighboring pixels on each side of the peak and fit a polynomial to the five points. The maximum value of this polynomial was used to locate the edge of the bar pattern at the sub-pixel level. This process was repeated

for each line of the image. After we processed each line, the mean sub-pixel value and standard error were stored for each bar edge located in each image.

We then measured the distance (in pixels) each bar edge shifted when we rotated the stage one degree in the same image set consisting of three to four images. This shift was 1017 to 1025 pixels depending upon the area of the detector (i.e., distance from the principal point). We only used bar edges whose position was estimated within 0.5 pixels (edge uncertainty after filtering = ± 0.05 ± 0.08 pixels). In all, we collected 242 measurements to derive the interior orientation parameters. Figure 2 documents how far the bars shifted with a one-degree rotation on the Ultradex rotary stage as a function of the distance from the left edge of the detector (sample). This line was then fit with a model to estimate the interior orientation parameters:

Principal Point ($x_{c,pix}$) = 1558 pixels (+22 pixel offset)

Focal Length (f) = 699.3 mm

Optical Distortion (k_2) = -1.741×10^{-5} (unitless)

These parameters can then be used to remove the optical distortion present in the system and map objects to the surface. First, we convert the pixel locations into units of mm from the edge of the detector:

$$x_d = x_{d,pix} * pitch$$

$$x_c = x_{c,pix} * pitch$$

where a pixel pitch of 0.012 mm/pix was used. Then, the radius of the observed pixel is calculated:

$$r = \text{abs}(x_d - x_c)$$

which is used to correct the pixel location (i.e., remove the optical distortion):

$$x_u - x_c = (x_d - x_c)(1 + k_2 r^2)$$

The undistorted location ($x_u - x_c$) is subsequently used along with the focal length and a simple pinhole camera model to project the image to the surface.

Further work from in-flight observations will enable more precise estimates of the absolute exterior orientation parameters (pointing of the instrument with respect to the spacecraft reference frame and any timing offsets).

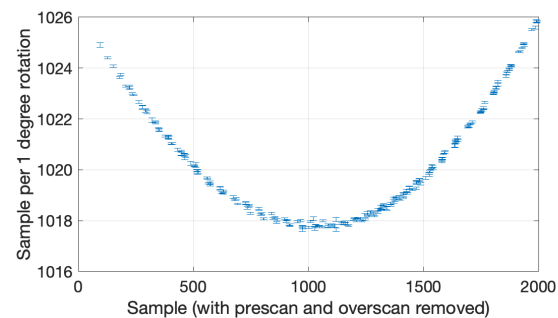


Figure 2: ShadowCam optical distortion.

References:

- [1] <https://www.nasa.gov/feature/kplo-ao>;
- [2] Robinson et al. (2010) Space Sci Rev.;
- [3] <https://www.hamamatsu.com/us/en/product/optical-sensors/image-sensor/cd-cmos-nmos-image-sensor/line-sensor/for-industry/S10202-08-01.html>